JOURNAL OF MATERIALS SCIENCE 24 (1989) 1281–1286

Structure and properties of thermoluminescent calcium fluoride glass-ceramic materials

I. GUTZOW, E. ZLATEVA, S. ANGELOV*, S. LEVY
*Institute of Physical Chemistry, and *Institute of General and Inorganic Chemistry, Bulgarian Academy of Sciences, Sofia 1040, Bulgaria*

New types of material for use in γ-dosimetry described here are glass-ceramics and silicate glass-ceramic enamels with thermoluminescent properties containing up to 30 wt% CaF_2 doped with MnO_2 and rare earth oxides. The structure and thermoluminescent properties of these materials have been investigated by applying a variety of complementary methods: X-ray analysis, electron microscopy, differential thermal analysis, electron paramagnetic resonance measurements and volume dilatometry. Thermal history, i.e. phase composition and degree of crystallinity, largely determines the thermoluminescent properties of the vitro-crystalline materials investigated. Optimal heat treatment favouring appropriate crystallization leads to a maximum in thermoluminescent intensity. Completely amorphous materials containing 20 to 30 wt% CaF_2 in the form of a glassy solution are devoid of any thermoluminescence. The thermoluminescent properties of natural fluorite are compared with those of synthetic materials.

1. Introduction

Glass-ceramic materials, offering a wide diversity of mechanical, optical and electrical properties are well known currently and they have found different applications in the modern technical world. The advantages of glass-ceramics as a material are that their properties average the properties of a large number of crystallites and that in most cases the residual glassy phase exerts a beneficial effect on the whole system. By combining different ratios of density, thermal dilatation, hardness of crystallites and ambient vitreous phase, materials with extreme mechanical properties can be obtained. Different glass-ceramic materials covering a wide range of optical and electrical properties have been developed in this way.

Powder-like and single-crystal materials with thermoluminescent properties, prepared on the basis of natural or doped synthetic CaF_2, have been widely used in radiation dosimetry [1–3]. In the preparation of single-crystal CaF_2 thermoluminescence dosimeters, the individual properties of the crystal are a decisive factor which determines to a great extent the characteristics of the whole device. The use of powdered materials has some disadvantages mainly due to the direct contact of the thermoluminescent material with air humidity and other aggressive environmental agents. A well established fact is that depending on the atmosphere where irradiation or thermoluminescence emission takes place, differing results can be obtained [3]. Therefore, different methods for the introduction of powdered CaF_2 in a protective matrix (e.g. organic binders, teflon, silicon rubber, etc.) have been proposed. Organic binders, however, have several shortcomings, e.g. they change colour during irradiation and heating, etc. In a previous paper, the synthesis of CaF_2 glass-ceramic thermoluminescent materials and of glass-ceramic silicate enamels was described [4]. It was found that these thermoluminescent enamels and glass-ceramics are not affected by atmospheric agents and humidity; moreover they are free from parasitic sensitivity to solar light, which limits the use of natural CaF_2 in dosimetry.

The present paper investigates the structure of such thermoluminescent vitreous-crystalline glass-ceramic materials, formed under different conditions, with special emphasis on the relationship between the thermoluminescent properties and structure. One of the main results obtained in the present study is that the thermoluminescent properties of the investigated silicate systems containing 10 to 30 wt% CaF_2 are observed only in materials where CaF_2 is crystalline. Samples containing CaF_2 as a glassy solution are totally devoid of thermoluminescent properties. A similar behaviour is to be expected, taking into consideration that investigations of the luminescent properties of various materials have shown that a relationship exists between the X-ray-induced photoluminescence and the structure and especially the glass-to-crystal ratio of different samples [5, 6]. As a result of our investigations, it appears that thermoluminescence can be used as an indicator of the particular structure of thermoluminescent materials. In addition to the synthetic materials mentioned, natural CaF_2 (fluorite) and synthetic CaF_2 with no dopants were also investigated.

2. Experimental details

Calcium fluoride was introduced into the boro-silicate enamel batches [4] at concentrations between 10 and 30 wt%, and the mixtures were melted in platinum crucibles at 1000° C. The dopants usually used [2, 3, 7] were manganese dioxide and rare earth element oxides. The following types of sample were used.

(a) Abrupt quenching of the melt by pouring it into

0022–2461/89 $03.00 + .12

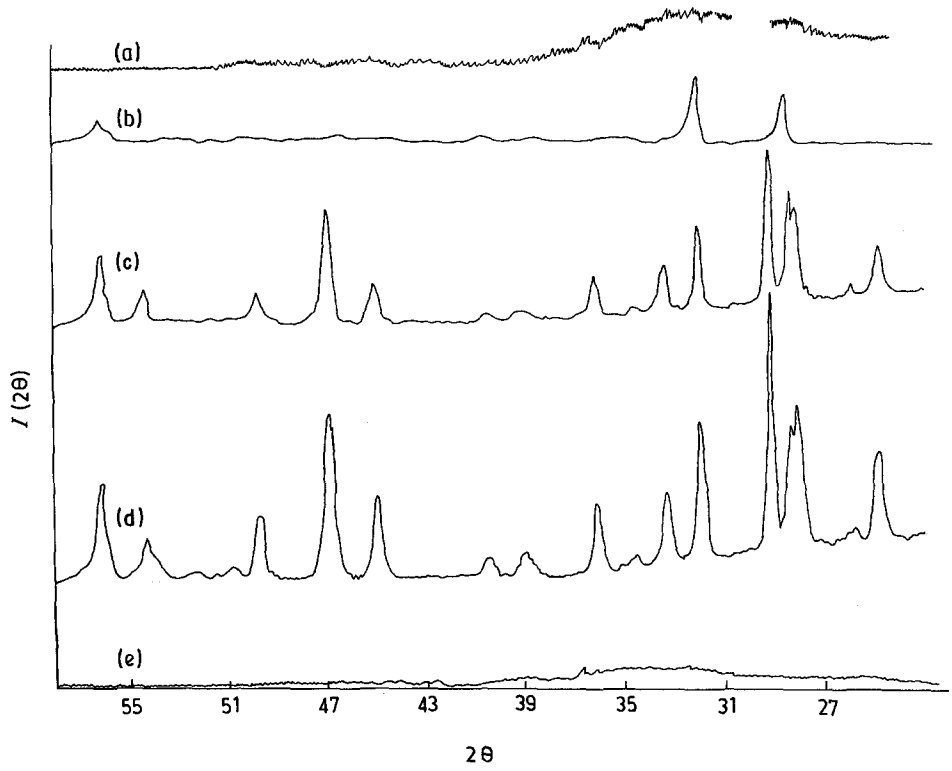

Figure 1 X-ray patterns of synthetic CaF_2 (A) samples. (a) Quenched, not subjected to thermal treatment; (b) thermally treated 30 min at 650° C, crystalline CaF_2 is formed; (c) thermally treated 30 min at 750° C, crystalline CaF_2 and cuspidine $CaF_2 \cdot 3CaO \cdot 2SiO_2$ are formed; (d) thermally treated 30 min at 850° C, increased amounts of crystalline CaF_2 and cuspidine are present; (e) crystalline sample, heat treated at 1000° C and rapidly quenched, the crystalline phases have melted.

the groove of a massive copper block made it possible to fix a CaF_2-rich phase as an amorphous segregate within the phase-separated glassy bulk of the samples. During the following thermal treatment of the phase-separated glass thus obtained, CaF_2 microcrystallites were formed. These samples are denoted CaF_2(A).

(b) Quenching of the melt in water (fritting) led to the direct formation of a CaF_2 crystalline phase embedded in the vitreous matrix (samples denoted CaF_2(B)).

In both cases, it was expected that after the segregation of CaF_2, the dopants present in the batch (and the melt) would be included in the segregated CaF_2-phase.

The amorphous structure of the quenched CaF_2(A) samples was proved by X-ray analysis (Fig. 1, curve a). They were subjected to additional isothermal heat treatment within the range 600 to 1000° C, quenched and again checked by X-ray analysis. Powdered samples of the abruptly quenched glass, of the thermally treated CaF_2(A) samples, as well as CaF_2(B) samples were subjected to γ-irradiation from a ^{60}Co source, and thermoluminescence glow-curves were obtained from each sample using a conventional thermoluminescence reader.

Bulk samples from the initial or thermally treated glass were used for the preparation of cross-cuts for optical microscopic investigations. In this way the basic methods applied in the present study were X-ray analysis, differential thermal analysis (DTA), optical and electron microscopy, as well as thermoluminescent

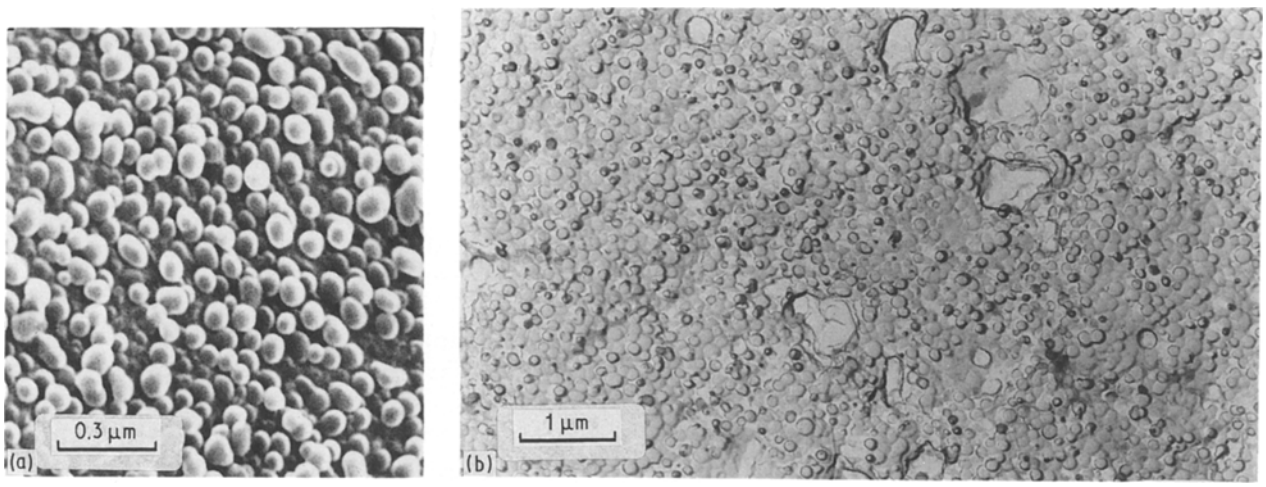

Figure 2 Scanning electron micrographs of liquid-phase separation in the matrix of quenched amorphous samples (a) and of initial stages of crystallization after 30 min heat treatment at 650° C (b). Surface of a freshly broken sample after 5 sec treatment with 2.5% hydrofluoric acid prior to SEM observation.

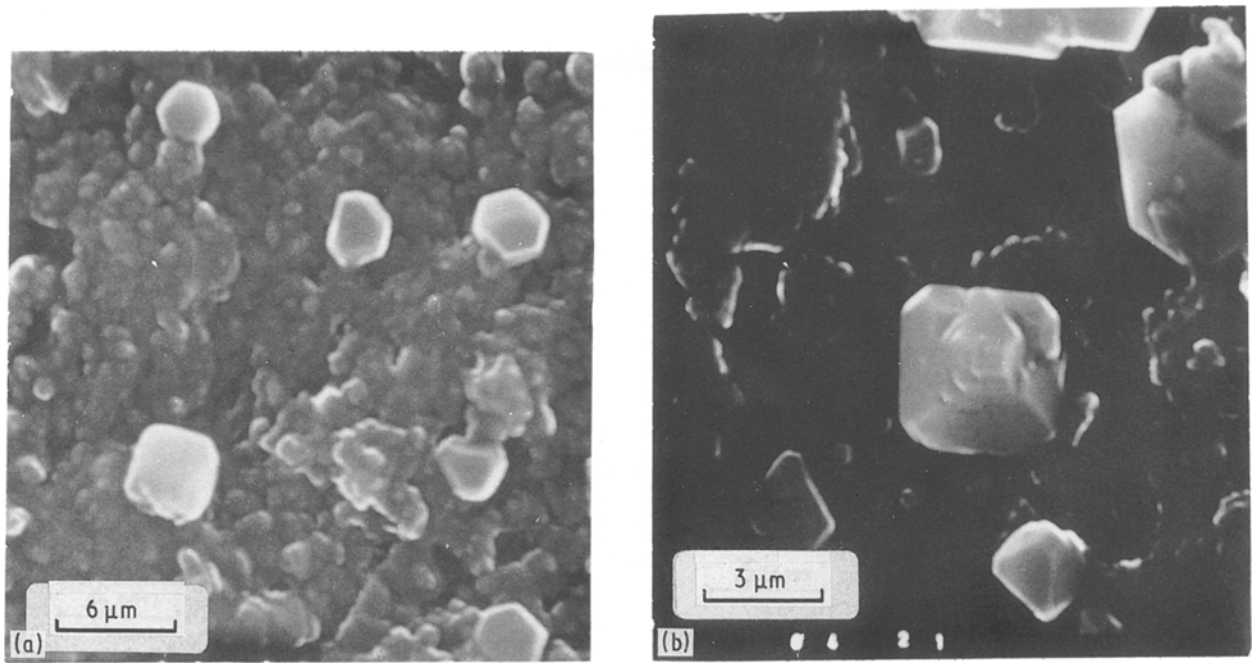

Figure 3 Scanning electron micrograph of CaF_2 (A) samples after 30 min heat treatment at 850° C. Cubic-octahedral CaF_2 microcrystallites are clearly visible in (a) and (b).

analysis, electron paramagnetic resonance (EPR) spectra and volumetric studies, the results of which are discussed in more detail below.

(c) Native fluorite samples (denoted CaF_2 (0)) have also been investigated. According to a thorough geochemical analysis [8] they contain substantial amounts of rare earth oxides and MnO_2.

(d) Finally, a.g. CaF_2 (Merck, p.a.) was used as blank samples, devoid of any dopants.

3. Results and discussion

The X-ray patterns of CaF_2(A) sample are shown in Fig. 1. The quenched samples, containing about 30% CaF_2 are amorphous (Fig. 1, curve a). Electron microscopy indicates that these quenched amorphous samples are phase-separated (Fig. 2a). Spherical droplets (0.2 μm diameter) are observed in the matrix. Upon heat treatment, CaF_2 crystals (evinced by X-ray analysis) appear between the droplets (Fig. 2b).

Calcium fluoride crystallites are initially formed upon heat treatment at temperatures above 650° C (Fig. 1, curve b). The crystallization of cuspidine ($Ca_4F_2Si_2O_7$), (Fig. 1, curve c) follows at 750° C. During the final stages of the recrystallization process (Fig. 1, curve d) well-shaped cubic-octahedric crystallites appear (Fig. 3a, b). With respect to the morphology, the latter display the typical CaF_2 crystal forms.

The DTA curve of an initially quenched CaF_2 (A) sample is shown in Fig. 4. The vitrification temperature is 570° C, within the range 600 to 900° C two crystal phases are separated, identified by X-ray analysis as fluorite (the exo-effect at 640° C) and cuspidine + CaF_2 (the exo-effect at 700° C), respectively. At higher temperatures the crystallites are melted (the endo-effects at 960 and 1050° C).

During isothermic heating of the samples within the temperature range 700 to 900° C, microcrystalline formations (as indicated by electron microscopy) grow linearly with time, reaching sizes up to approximately 5 μm (Fig. 5).

It was established that the quenched amorphous CaF_2 (A) samples, regardless of the fact that they are doped, even after heavy irradiation with 1 500 to 35 000 R, do not display thermoluminescent properties (Fig. 6). After 30 min thermal treatment, specified in the figure, thermoluminescence typical of Mn- and RE-doped calcium fluoride appears, reaching a maximum when thermal treatment before irradiation is carried out at 850° C. In the case of molten (and secondary quenched) samples, where CaF_2 reappears as a vitreous solution, thermoluminescence is again absent.

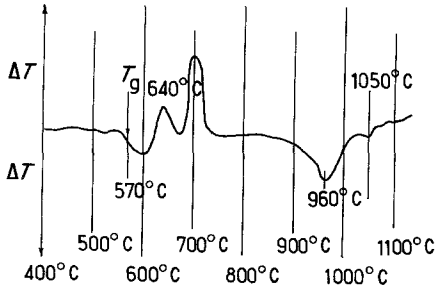

Figure 4 DTA of CaF_2 (A) samples at a scanning rate of 7.5° C min^{-1}. Exo-effects at 640 and 700° C; formation of CaF_2 and cuspidine. Endo-effects: melting of the crystalline phases.

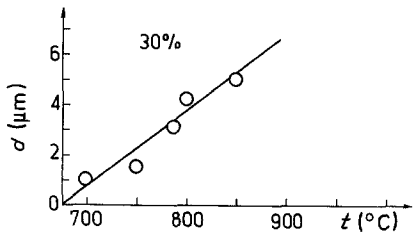

Figure 5 Alteration of the average size $\bar{d}$ (μm) of CaF_2 crystallites depending on temperature of the 30 min heat treatment of the quenched CaF_2 samples.

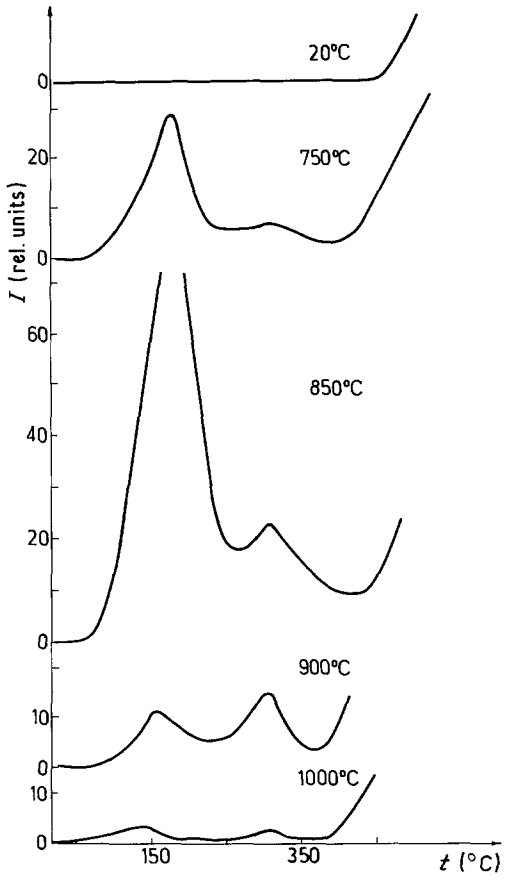

Figure 6 Glow curves of CaF_2 (A) samples. Thermoluminescence intensity, I (relative units) is plotted against temperature (° C) of the sample. Samples irradiated with a ^{60}Co source at 1500 R. Temperature of initial heat treatment indicated as parameter in ° C.

Data for the structure and properties of the fritted thermoluminescent enamel material (samples CaF_2(B)) are shown in the following figures. Fig. 7 gives the X-ray pattern of the single CaF_2 crystalline phase, formed in the CaF_2(B) samples upon direct fritting.

The DTA curve of a CaF_2 (B) sample is shown in Fig. 8. The exo-effect observed at 700° C, according to X-ray structural data, corresponds to the additional formation of crystalline CaF_2, while the endo-effect at 880° C reflects the melting temperature.

Electron microscopic results on the structure of the thermoluminescent enamel, sample CaF_2 (B), are shown in Fig. 9. The size of the CaF_2 crystallites distributed within the bulk of the glass is about 1 μm.

The room temperature EPR spectra of different synthetic samples of pure, undoped CaF_2, of quenched and of heat-treated CaF_2(A) and of fritted CaF_2(B) are presented in Fig. 10. The figure shows that (1)

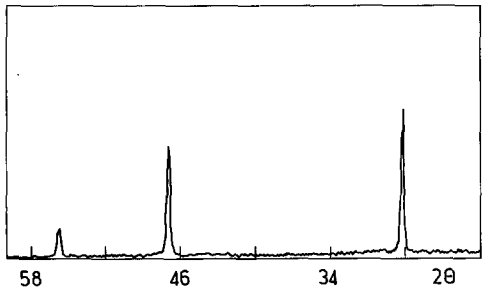

Figure 7 X-ray pattern of CaF_2 (B) samples after fritting. Crystalline CaF_2 is formed.

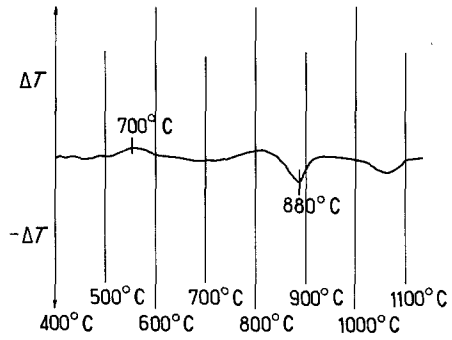

Figure 8 DTA of fritted CaF_2 (B) samples at a heating rate of 7.5° C min^{-1}. The exo-effect at 700° C corresponds to the additional formation of crystalline CaF_2, while the endo-effect at 880° C indicates its melting point.

undoped CaF_2 (powders) give no EPR signal for Mn^{2+}; (2) quenched CaF_2(A) samples display a considerably weaker Mn^{2+} signal compared to CaF_2 (B) (curve 4), both containing identical amounts of MnO_2. This is due, probably, to the fact that Mn^{2+} ions in CaF_2 (A) samples occupy lattice sites with lower local symmetry; (3) when CaF_2 (A) samples are thermally treated at 850° C for 30 min, the EPR signal does not evince any substantial changes compared to the preceding case; (4) CaF_2(B) samples fritted (in water) display a signal corresponding to hydrated Mn^{2+} thus providing evidence that water has access to the sites occupied by Mn^{2+}, forming hydrated complexes (the typical sextet with a g-value approximately equal to 2); (5) undoped CaF_2 samples (the same as in

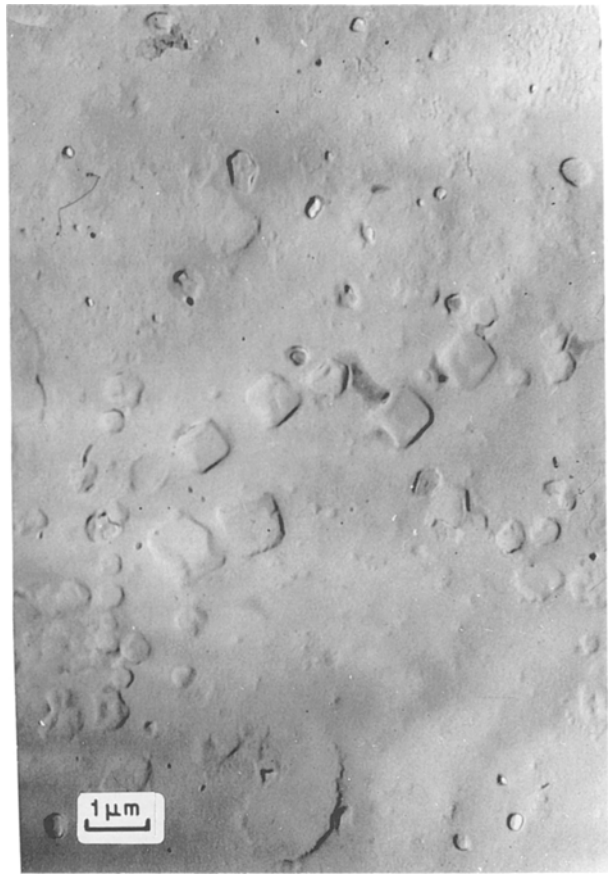

Figure 9 Transmission electron micrograph of fritted CaF_2 (B) using a Pt/C replica from the freshly broken sample. CaF_2 crystallites are visible.

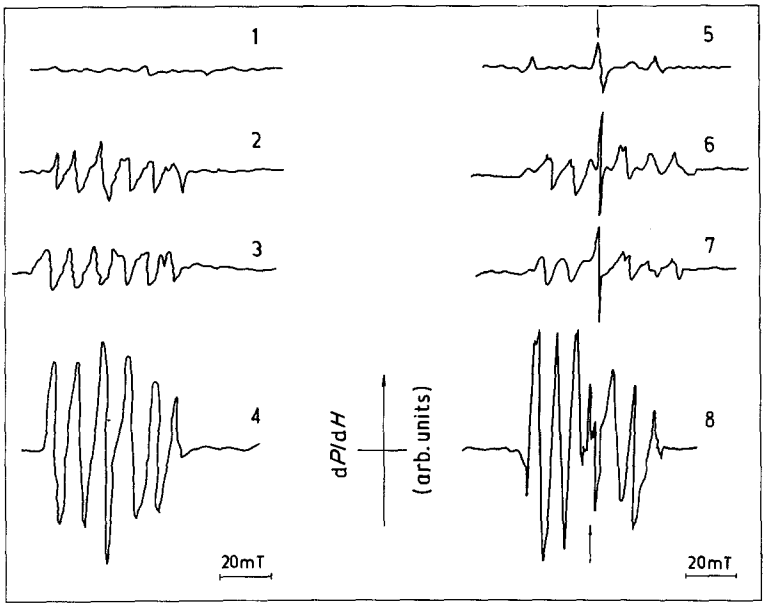

Figure 10 EPR spectra of different CaF_2 materials. Left-hand side spectral, samples not subjected to irradiation: (1) undoped, synthetic analytical grade CaF_2 powder; (2) quenched glassy CaF_2 (A) samples, not subjected to thermal treatment; (3) crystalline CaF_2 (A) sample, thermally treated 30 min at 850° C; (4) crystalline fritted CaF_2 (B) sample. Right-hand side, the same samples as on the left but all samples subjected to γ-irradiation from a ^{60}Co source at 20×10^3 R.

(1) above), containing no dopants, after irradiation display a radiation defect with a g-value of about 2; (6) quenched amorphous CaF_2 (A) samples, not subjected to thermal treatment display an analogous radiation defect; (7) quenched CaF_2 (A) samples, treated for 30 min at 850° C; as well as (8) quenched CaF_2 (B) samples, not subjected to thermal treatment, display the same radiation defects.

It is important to note that the irradiation defects are observed in all doped samples, regardless of whether or not they display thermoluminescence. This means that the above mentioned defect is not related to thermoluminescent active traps. The EPR signal curves of native calcium fluoride, denoted $CaF_2(0)$, are shown in Fig. 11. It is seen that native samples of $CaF_2(0)$ not subjected to irradiation and heated for 1 h at 350° C display an EPR spectrum with a g-factor of 2, which can be considered a residual, naturally existing radiation defect (due to natural radioactivity). It is evident, that $CaF_2(0)$ samples subjected to additional γ-irradiation from a ^{60}Co source with 20×10^3 R, display an increase of the signal related to the above-mentioned defect. In addition, in native CaF_2, a clear-cut Mn^{2+} signal appears with the characteristic sextet hyper-fine structure and g-factor of 2, similar to that observed in the case of the CaF_2 (B) samples.

It is well known that in the case of powdered samples, only the transmission $m_s = -1/2 \rightarrow +1/2$ (m_s = spin quantum number) is registered, its intensity being lower in less symmetrical fields.

This property of Mn^{2+} renders it a very helpful "sensor" for investigation of the local symmetry at sites which these ions occupy in the CaF_2 lattice. In all the samples, the Mn^{2+} signal appears with a g-factor approximately equal to 2 and the characteristic sextet structure.

In dopant-free samples there is no Mn^{2+} EPR signal. However, the same radiation defects are observed in all samples (doped and undoped), suggesting that they are not related to any dopant or thermoluminescent traps.

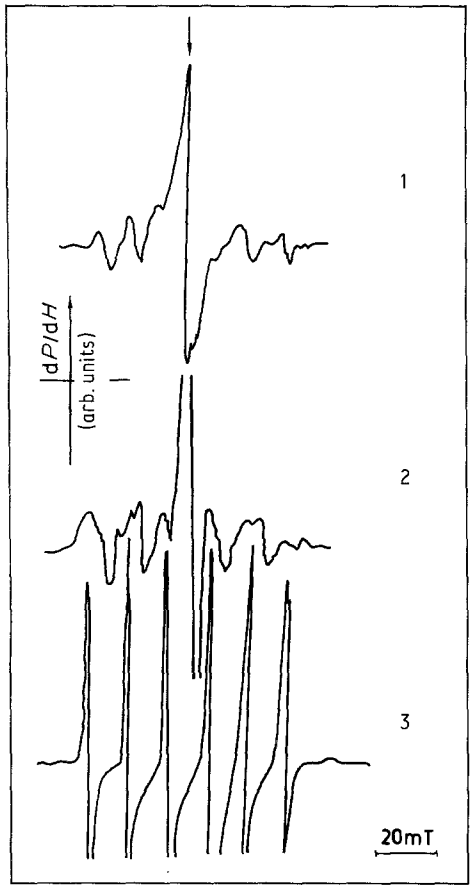

Figure 11 EPR spectra of samples of native $CaF_2(0)$. (1) Thermally treated 1 h at 350° C not subjected to irradiation; (2) the same sample, but γ-irradiated with a ^{60}Co source at 20×10^3 R and heat treated in the same way as (1); (3) test substance, blend of Mn^{2+} in powdered MgO (non-irradiated sample).

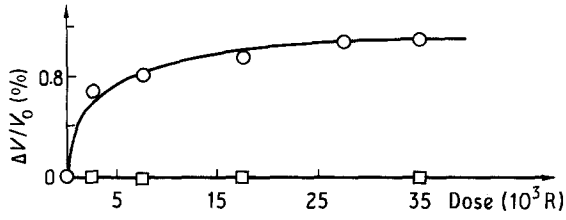

Figure 12 Percentage alteration of the relative volume, $\Delta V/V_0$, of CaF_2 (A) samples after irradiation with γ-^{60}Co, at doses indicated on the abscissa.

In addition to the Mn^{2+} signal, the synthetic samples display a weak Fe^{3+} signal with a g-factor of about 4 (not shown in Fig. 11) probably due to contamination of the quartz sand used in the synthesis of our materials.

An additional volumetric investigation [9] was carried out, in an effort to establish structural changes related to the γ-irradiation of our Mn-doped CaF_2 materials. These investigations were carried out using a highly sensitive volumetric method [9]. It was found that quenched CaF_2 (A) glass samples which do not display thermoluminescence, show no changes in their density. In contrast, thermally treated CaF_2 (A) samples show a measurable alteration of their density during irradiation, Fig. 12.

4. Conclusions

The investigations show the relationship between thermoluminescence, genesis and structure of a typical thermoluminescent material, which can be described as a glass-ceramic. The phase-separated glassy material displays no thermoluminescence, regardless of the fact that it contains substantial amounts of amorphous CaF_2 and an adequate quantity of dopant. The existence of amorphous thermoluminescent materials, e.g. alumo-silicate glasses activated by terbium dopants is well known [10]. In our case the thermoluminescent properties emerge only after the appearance of electron-microscopically observable CaF_2 crystallites. Presumably the optimum thermoluminescence values are connected with a preferred, highly ordered structure of the crystals and the dopants they contain. Thus, thermoluminescent glass-ceramic materials are an example for the structural variety which can be achieved by the glassy-crystalline systems and they provide evidence showing how similar structures can be the source of different properties.

References

1. K. K. SHWARZ, Z. A. GRANT, T. K. MEZHS and M. M. GRUBE, "Thermolumynesszentnaya dosimetriya" (Izd. Znanie, Riga, 1968) p. 37.
2. M. FRANK and W. STOLZ, "Festkörperdosimetrie ionisirender Strahlung" (Teubner, Leipzig, 1969) p. 80.
3. J. R. CAMERON, N. SUNTHRALINGMAN and G. N. KENNEY, "Thermoluminescent Dosimetry", (University of Wisconsin Press, Madison, Milwaukee, London, 1968).
4. I. GUTZOW, E. ZLATEVA, D. DOBREV, M. ATANASOV, K. SAKHNO, *Izv. Chim. Bulg. Acad. Sci.* (1987) in print.
5. G. BODEN and W. NOWAK, *Silikattechnik* **28** (1977) 166.
6. G. BODEN, *Z. Chem.* **19** (1979) 184.
7. F. DANIELS, T. BOYD and D. SINDERS, *Uspekhi fiz. Nauk* **51** (1953) 271.
8. E. ALEKSIEV and M. PAVLOVA, *Bulg. Akad. Sci.* **14** (1967) 17.
9. E. ZLATEVA and I. GUTZOW, *Phys. Status Solidi* (a) **107** (1988) K99.
10. S. M. BREKHOVSKIKH, J. M. VIKTOROVA, J. L. GRINSTEIN and L. M. LANDA, "Osnovy Radiatsionnogo Materialovedenya Stekla i Keramiki" (Izd. Lit. po stroitel' stvu, Moscow, 1971) p. 171.

Received 7 March
and accepted 25 July 1988